MOLECULAR AND CELLULAR BIOLOGY, May 2006, p. 3864–3874 Vol. 26, No. 10
0270-7306/06/$08.00+0 doi:10.1128/MCB.26.10.3864–3874.2006

Protein Methyltransferase 2 Inhibits NF-κB Function and Promotes Apoptosis†

Lakshmanan Ganesh,[1]‡ Takanobu Yoshimoto,[2]‡§ Narayani C. Moorthy,[1]¶ Wataru Akahata,[1] Manfred Boehm,[2,3] Elizabeth G. Nabel,[2] and Gary J. Nabel[1]*

Vaccine Research Center, National Institute of Allergy and Infectious Diseases, National Institutes of Health, Building 40, Room 4502, 40 Convent Dr., Bethesda, Maryland 20892-3005,[1] National Heart, Lung, and Blood Institute, National Institutes of Health, Building 31, Room 5A48, 31 Center Dr.,[2] and Hatfield Clinical Research Center, Building 10 CRC, Room 5E-3132, 10 Center Dr.,[3] Bethesda, Maryland 20892

Received 29 November 2005/Returned for modification 18 December 2005/Accepted 18 February 2006

The protein arginine methyltransferases (PRMTs) include a family of proteins with related putative methyltransferase domains that modify chromatin and regulate cellular transcription. Although some family members, PRMT1 and PRMT4, have been implicated in transcriptional modulation or intracellular signaling, the roles of other PRMTs in diverse cellular processes have not been fully established. Here, we report that PRMT2 inhibits NF-κB-dependent transcription and promotes apoptosis. PRMT2 exerted this effect by blocking nuclear export of IκB-α through a leptomycin-sensitive pathway, increasing nuclear IκB-α and decreasing NF-κB DNA binding. The highly conserved *S*-adenosylmethionine-binding domain of PRMT2 mediated this effect. PRMT2 also rendered cells susceptible to apoptosis by cytokines or cytotoxic drugs, likely due to its effects on NF-κB. Mouse embryo fibroblasts from PRMT2 genetic knockouts showed elevated NF-κB activity and decreased susceptibility to apoptosis compared to wild-type or complemented cells. Taken together, these data suggest that PRMT2 inhibits cell activation and promotes programmed cell death through this NF-κB-dependent mechanism.

NF-κB is sequestered in the cytoplasm by an IκB complex (5, 8, 26, 45, 52), and phosphorylation of IκB in this complex by two inducible kinases, IκB kinase 1 (IKK1) and IKK2, leads to subsequent ubiquitination and degradation of these proteins by the 26S proteasome (58, 59). The released NF-κB then translocates to the nucleus, where it stimulates the synthesis of genes involved in immune and inflammatory responses (25) by formation of a higher-order transcription complex involving two key multiple coactivators, histone-acetyltransferase p300 and its homolog, the CREB-binding protein (CBP) (1, 19, 22, 35, 36, 39). These coactivators promote the rapid formation of the preinitiation and reinitiation complexes by bridging NF-κB to the basal transcriptional machinery and facilitating multiple rounds of transcription (20). NF-κB DNA binding and NF-κB-dependent transcription are attenuated by newly synthesized IκB-α in the nucleus, where it associates with NF-κB/RelA complexes. As newly synthesized IκB-α accumulates in the nucleus, there is a progressive reduction of both NF-κB DNA binding and NF-κB-dependent transcription (4), presumably by export of NF-κB-IκB-α complexes from the nucleus (3, 42, 49).

N-methylation of proteins at arginine residues is catalyzed by the protein arginine methyltransferase (PRMT) family (18). PRMTs can be divided into two major classes, based on the type of dimethyl arginines they generate: type I PRMTs catalyze the formation of asymmetric dimethyl arginines, while type II PRMTs form symmetric dimethyl arginines. Among the seven arginine methyltransferases (10, 16, 21, 29, 32, 40, 43, 50), only PRMT5 and PRMT7 are known to catalyze the formation of symmetric dimethyl arginines. PRMT1, -2, and -3 are similar to one another (Fig. 1A, left) and share an *S*-adenosylmethionine (Ado-Met)-binding motif related to those found in nucleic acid and small-molecule methyltransferases (24) and in other less homologous protein methyltransferases. Some of these protein methyltransferases have now been implicated in RNA processing and/or nucleocytoplasmic transport, receptor-mediated signaling, and transcriptional regulation (2), for example, by methylation of coactivators or histones (6, 55, 57).

PRMT2 was shown to be an estrogen receptor alpha coactivator (41), although the substrates of PRMT2 methylation are still unknown (43, 50). Recently PRMT4 (CARM1) was shown to synergistically coactivate NF-κB-mediated transcription by forming a complex with p300 and NF-κB in vivo (12). Since PRMT4 is capable of forming a complex with NF-κB, we tested whether PRMT1, PRMT2, and PRMT3 participate in NF-κB-dependent gene activation. Here, we show that, in contrast to PRMT4, PRMT2 inhibits NF-κB-dependent transcription. PRMT2 exerts this effect by causing nuclear accumulation of IκB-α, which concomitantly decreases nuclear NF-κB DNA binding. Mouse embryo fibroblasts (MEFs) from PRMT2 genetic knockouts show decreased levels of nuclear IκB-α, increased NF-κB activity, and decreased susceptibility to apop-

* Corresponding author. Mailing address: Vaccine Research Center, National Institute of Allergy and Infectious Diseases, National Institutes of Health, Building 40, Room 4502, 40 Convent Dr., Bethesda, MD 20892-3005. Phone: (301) 496-1852. Fax: (301) 480-0274. E-mail: gnabel@nih.gov.

† Supplemental material for this article may be found at http://mcb.asm.org/.

‡ These authors contributed equally to this work.

§ Present address: Department of Clinical and Molecular Endocrinology, Tokyo Medical and Dental University, 1-5-45 Yushima, Bunkyo-ku, Tokyo 113-8519, Japan.

¶ Present address: 21 Murrays Gate Rd., Chennai 600018, India.

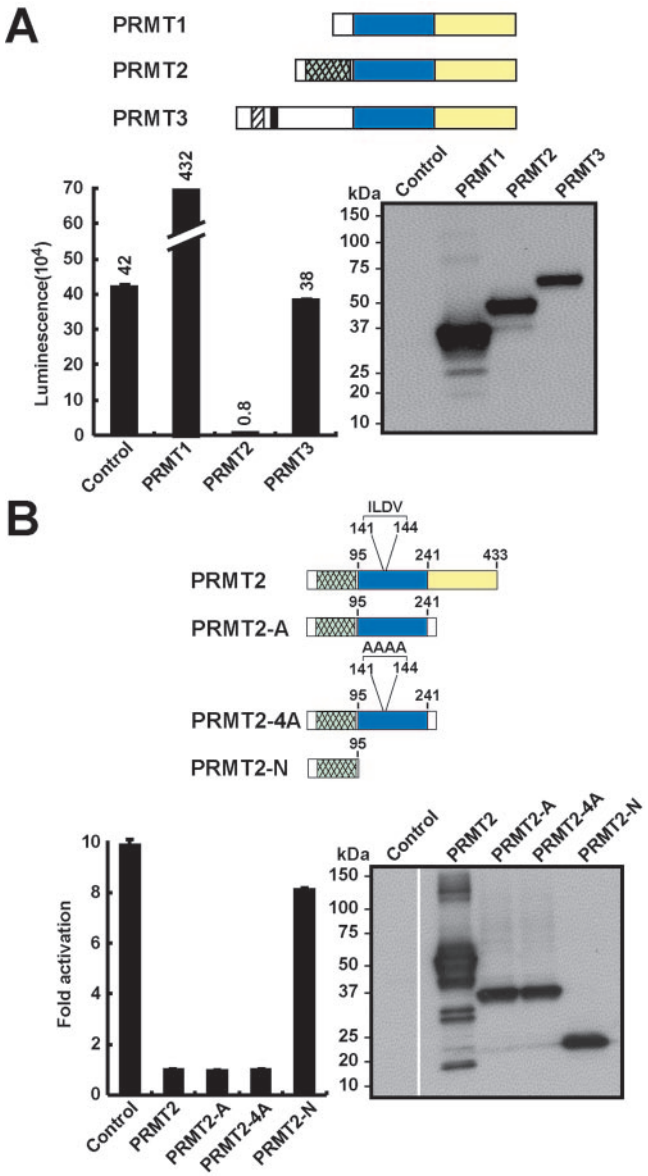

FIG. 1. PRMT2 inhibits HIV-1 transcription in contrast to other arginine methyltransferases and requires its methyltransferase domain. (A) PRMT2 inhibits transcription in contrast to other methyltransferases. (Top) Human PRMT1, -2, and -3 structures share a core arginine methyltransferase region, composed of an Ado-Met-binding domain (blue) and divergent C-terminal domain (yellow). (Bottom left) 293T cells were transfected with 100 ng of 5κB-luciferase reporter and 1 μg of methyltransferase expression constructs as indicated, and luciferase activity was measured (Materials and Methods). (Bottom right) A total of 15 μg of protein from each extract was run on a 4 to 15% polyacrylamide gel and transferred to a PVDF membrane. Western blotting was performed with a mouse anti-HA antibody. (B) Deletion of the methyltransferase domain abolishes PRMT2 inhibition of transcription. (Top) Schematic representation of PRMT2 and PRMT2 mutants. Amino acids 141 to 144 (ILDV) represent the Ado-Met consensus site in all PRMT family members. The Ado-Met consensus site in PRMT2 was mutated and replaced by four alanines (PRMT2-4A). PRMT2-A is an alternative splice variant of PRMT2 and lacks the divergent COOH terminus found in other PRMT family members. PRMT2-N contains the first 95 amino acids of PRMT2. (Bottom left) 293T cells were transfected with 1 μg of HA-tagged PRMT2, PRMT2-A, PRMT2-4A, and PRMT2-N and 100 ng of 5κB-luciferase reporter. Cell lysates were collected 48 h after transfection, and luciferase activity was assayed (Materials and Methods). (Bottom right) A total of 15 μg of protein from each extract was run on a 4 to 15% polyacrylamide gel and transferred to a PVDF membrane. Western blotting was performed with a mouse anti-HA antibody.

tosis compared to wild-type (WT) or complemented PRMT2-transfected knockout cells. These findings indicate that PRMT2 negatively regulates cell activation and promotes programmed cell death.

MATERIALS AND METHODS

Plasmids. The human immunodeficiency virus type 1 (HIV-1)–luciferase (Luc) reporters, WT and mutant, have all been described previously (17, 31, 34, 37). The Rous sarcoma virus (RSV) expression plasmids containing the p50 and p65 cDNAs have also been previously described (15). The human PRMT1, PRMT2, and PRMT3 cDNAs were cloned by reverse transcription-PCR using total RNA extracted from Jurkat cells. PRMT2-A, an alternative splice variant of PRMT2 (27), was cloned by PCR using a human B-cell library as template. The following primer pairs were used for PCR: 5′-AAGTCGACGCCATGGCAACATCAGGTGACTGT-3′ and 5′-AAGCGGCCGCTTATCTCCAGATGGGGAAGACTT-3′ for human PRMT2, 5′-AAGGATCCGCGAACTGCATCATGGAGAA-3′ and 5′-AAAAGCTTAAACCGCCTAGGAACGCTCA-3′ for human PRMT1, 5′-AAGATATCGCCATGGACGAGCCAGAACTGTCGGACAGCGGGGACGAGGCCGCCTGGGAGGATGAGGACGAT-3′ and 5′-AATCTAGATTACTGGAGACCATAAGTTTGAGTTG-3′ for human PRMT3, and 5′-AAGTCGACGCCATGGCAACATCAGGTGACTGT-3′ and 5′-AATCTAGATTAAAATGAATCACGCACGACCCTT-3′ for PRMT2-A. All these coding regions of cDNA were subcloned into the pVR1012 mammalian expression vector (13) with a hemagglutinin (HA) tag at the C terminus. The four-alanine mutant of PRMT2 (PRMT2-4A) was generated from the wild-type pVR1012 PRMT2 construct using the Stratagene QuikChange site-directed mutagenesis kit according to the manufacturer's directions. The sequence of the sense mutagenic oligonucleotide used is 5′-AATAAAGAATCCCTGACGGATAAAGCCGCAGCCGCGGTGGGCTGTGGGACTGGGATCATC-3′. This mutation introduced a unique SacII site within the PRMT2 sequence. Mutant clones were identified by restriction of the isolated plasmid DNA with SacII and verified by sequencing. The PRMT2-N (PRMT2, 1 to 95 amino acids) mutant was generated from the wild-type pVR1012 PRMT2 construct by PCR using the primer pairs 5′-GCGCGCGATATCGCCATGGCAACATCAGGTGACTGT-3′ and 5′-GCGCGCTCTAGACTAGGCATAGTCAGGCACGTCATAAGGATAGGGGTCGTACTCATCCACGT-3′. Wild-type PRMT2-A was subcloned into pGEX-6P (Amersham Pharmacia) for the generation of glutathione-*S*-transferase (GST) fusion proteins. The luciferase reporter 5κB-Luc was purchased from Stratagene. The expression vector for the IκB-α mutant (S32A/S36A) was described previously (56).

A wild-type IKK2 expression plasmid was used as a template to create a constitutively active mutant by replacement of two serine residues at amino acids 177 and 181 by glutamic acid by site-directed mutagenesis (Stratagene): 5′-GAGCTGGATCAGGGCGAGCTCTGCACAGAATTCGTGGGGACCCTG-3′ and 5′-CAGGGTCCCCACGAATTCTGTGCAGAGCTCGCCCTGATCCAGCTC-3′ (47). The resulting constitutively active IKK2 fragment was amplified by PCR and cloned into an RSV expression vector. The RSV expression vector was created by replacing the cytomegalovirus promoter in the pVR1012 vector with an RSV promoter.

Cell culture, transfection, and reporter gene assays. The E1A-transformed human kidney cell line 293 and NIH 3T3 cells were maintained in Dulbecco's modified Eagle medium supplemented with 10% fetal calf serum (FCS) and penicillin-streptomycin at 37°C in 5% carbon dioxide in tissue culture dishes. *prmt2*$^{-/-}$ MEFs (unpublished data) and wild-type MEFs were prepared from day 13.5 embryos and maintained in Dulbecco's modified Eagle medium supplemented with 10% FCS. MEFs at passage 4 were used in the experiment described in this paper. Lipofectamine Plus reagent (Boehringer Mannheim) was used to transfect both 293 and NIH 3T3 cells according to directions from the manufacturer. The transfection efficiency of both 293 and NIH 3T3 cells using Lipofectamine Plus reagent was found to be constant and reproducible, with standard deviations of ~10% as assayed by β-galactosidase assays and fluorescence-activated cell sorter analysis of a cotransfected CD2 expression vector. Tumor necrosis factor alpha (TNF-α) stimulation of cells was done using recom-

binant human TNF-α (200 U/ml; Peprotech) for 12 h. Transfected cells were harvested at 36 h for luciferase assays. To analyze the κB reporter activity in MEFs, cells were transfected with the reporter (5κB-Luc) and PRL-TK vector (Promega) using FuGENE6 transfection reagent (Roche). Luciferase activity was analyzed with the luciferase reporter assay system (Promega). The results of all luciferase experiments are an average of three independent experiments, each conducted in triplicate; values are corrected for transfection efficiency.

DNA-binding assay. Electrophoretic mobility shift assays (EMSAs) were conducted on 10 μg of nuclear extract protein from 293 cells transiently transfected with pRSV p50/p65 expression constructs and pVR1012 PRMT2/PRMT2-N expression constructs. A modified Dignam procedure (14) was used to prepare nuclear extracts from 293 cells (39). NF-κB DNA binding was assayed with a double-stranded ^{32}P-labeled κB probe (Geneka Biotechnology). DNA-binding assays were performed as described previously (39). Supershifting was done using NF-κB p65 (C-20) and NF-κB p50 (H-119) (Santa Cruz). GST-PRMT2 fusion proteins were expressed in BL21(DE3) cells, and extracts were prepared as described previously (46).

To determine if PRMT2 interfered with the dimerization of p50/p65, immunoprecipitations were carried out in immunoprecipitation (IP) buffer (20 mM HEPES, 150 mM KCl, 100 mM NaCl, 2.5 mM $MgCl_2$, 0.5% NP-40, 1 mM dithiothreitol, protease inhibitor cocktail [Complete; Boehringer Mannheim]) using α-p65 antibody-conjugated beads (p65 AC; Santa Cruz) from 293 nuclear extracts that had been transfected with either PRMT2 or PRMT2-N. The complexes were resolved by 4 to 15% sodium dodecyl sulfate-polyacrylamide gel electrophoresis (SDS-PAGE) and transferred to polyvinylidene difluoride (PVDF) membranes. p50 was detected by Western blotting with a p50 antibody (H-119; Santa Cruz).

Small-scale preparation of nuclear extracts. A modified Dignam procedure (14) was used to prepare nuclear extracts from 293 cells. Cells were harvested, washed with phosphate-buffered saline (PBS), resuspended in 1 ml of Dignam buffer A, and transferred to prechilled microfuge tubes, which were spun at 1,000 rpm for 1 min. The supernatant was aspirated thoroughly, and pellets were carefully resuspended to avoid frothing, in 60 μl of modified Dignam buffer A containing 0.1% NP-40. Samples were incubated at 4°C for approximately 10 min, and microcentrifuged for 10 min at 4°C. The cytoplasmic extract supernatant was diluted in 3 volumes of modified Dignam buffer D and frozen quickly. The pellets were resuspended in 40 μl Dignam buffer C. Samples were incubated for 15 min at 4°C on a tumbler and centrifuged again for 5 min at 4°C. The supernatant was diluted with 6 volumes of modified Dignam buffer D. Samples were frozen quickly in aliquots and stored at −70°C.

Fusion proteins. GST proteins were expressed in BL21(DE3) cells, and extracts were prepared in accordance with previously published methods (46). GST fusion proteins were purified using glutathione-Sepharose beads (Pharmacia) and washed three times with IP buffer.

Western blotting. Proteins resolved by SDS-PAGE were transferred to PVDF membranes. Membranes were blocked with 5% nonfat dry milk and 2.5% bovine serum albumin (BSA) in Tris-buffered saline (TBS) containing 0.5% Tween 20 (TBS-Tween) for 10 min at room temperature and then incubated with primary antibody in TBS-Tween–milk–BSA for 1 to 2 h at room temperature or overnight at 4°C. Following three 15-min washes in TBS-Tween, membranes were incubated for 1 h with the appropriate horseradish peroxidase-conjugated secondary antibody (Santa Cruz) in TBS-Tween–milk–BSA. After two more washes in TBS-Tween and a rinse in PBS, the immunoreactive proteins were visualized by enhanced chemiluminescence (Amersham).

In vitro association assay. To determine whether PRMT2 interfered with the dimerization of p50/p65, immunoprecipitations were carried out in IP buffer using α-p65 antibody-conjugated beads (p65AC; Santa Cruz) from 293 nuclear extracts that had been transfected with either PRMT2 or PRMT2-N. The complexes were resolved by 4 to 15% SDS-PAGE and transferred to PVDF membranes. p50 was detected by Western blotting with a p50 antibody (H-119; Santa Cruz). For binding of p65 to p300/TAF_{II}250, immunoprecipitations were carried out using either a p300 NH_2-terminal antibody (NM11; Pharmingen) or the TAF_{II}250antibody (6B3; Santa Cruz) from 293 nuclear extracts that had been transfected with either PRMT2 or PRMT2-N. p65 was detected by Western blotting with a p65 antibody (Santa Cruz).

For binding of GST-methyltransferase proteins to NF-κB, pBluescript constructs of p50/p65 were transcribed and translated in vitro with the TNT-T7-coupled reticulocyte lysate system (Promega) with [^{35}S]methionine (Amersham Pharmacia) in accordance with the manufacturer's instructions. A 10-μl volume of the reaction product was incubated in IP buffer with purified GST-methyltransferase proteins. Typically, 0.5 μg, 1 μg, and 2 μg (each) of GST and GST-PRMT2 are used in these assays. After incubation at 4°C for 1 h, the beads were washed three times with IP buffer. The bound proteins were solubilized in SDS sample buffer, subjected to SDS-PAGE, and visualized by autoradiography.

In vitro methyltransferase reactions. In vitro methyltransferase reactions were carried out as described previously (10). Mixed calf thymus histones (Boehringer Mannheim) were incubated for 30 min at 30°C in 30-μl reaction mixtures containing 20 mM Tris-HCl, 0.2 M NaCl, and 4 mM EDTA (pH 8.0); 10 pg mixed histones; PRMT1 and/or PRMT2 immunoprecipitated from 100 μg transfected 293 whole-cell-extract protein; and 7 μM *S*-adenosyl-L-[*methyl*-^{3}H]methionine (specific activity,14.7 Ci/mmol). Reactions were stopped by the addition of SDS-PAGE sample buffer. The reactions were then subjected to SDS-PAGE on 10 to 20% Tris-HCl gradient gels (Bio-Rad). Gels were stained with Coomassie blue to visualize histone bands, and then the incorporated label was enhanced using Enhance (NEN Life Sciences) and subjected to fluorography for 1 to 5 days at −70°C on sensitized Kodak Biomax film. Film images were digitized using a scanner equipped with a film-scanning unit. Bands were quantified using Imagequant software.

Immunohistochemistry and confocal microscopy. *prmt2*$^{-/-}$ fibroblasts were transfected with an HA-tagged PRMT2 expression vector. At 36 h after transfection, the cells were treated with TNF-α for 30 min. The medium was then removed, and cells were incubated for an additional 30 min in the presence or absence of leptomycin B (LMB). Cells were fixed, permeablized with CytoFix-CytoPerm (BD Biosciences) for 20 min, and washed with Perm/Wash buffer (BD Biosciences). IκB-α (rabbit polyclonal antibody, 1:1000; Santa Cruz Biotechnology) and HA (rat monoclonal antibody, 1:500; Roche) were diluted in Perm/Wash buffer and incubated for 1 h. After two washes, cells were stained with anti-rabbit Alexa 488 and anti-rat Alexa 564 (1:1,000; Invitrogen) for 30 min. Cells were washed and mounted with Ultracruz mounting medium (Santa Cruz) containing DAPI (4′,6′-diamidino-2-phenylindole). Confocal microscopy was performed using a Leica confocal microscope.

Apoptosis analysis. Apoptosis in PRMT2-expressing 293 cells was analyzed as follows. Cells were seeded at 2.5×10^5 per well in six-well plates. The next day, empty vector, mutant IκB-α (S32A/S36A), or PRMT2 was cotransfected with CD2 expression vector. Twenty-four hours after transfection, cells were stimulated with TNF-α (1,000 U/ml) for 24 h. Both floating and attached cells in each well were harvested by EDTA treatment. Cells were stained with antigen-presenting cell-labeled anti-CD2 antibody (BD Biosciences) in SM buffer (PBS containing 2% FCS). After being washed twice with PBS, cells were stained with fluorescein isothiocyanate (FITC)-labeled annexin V and propidium iodide with the Annexin V FITC Apoptosis Detection kit (Calbiochem) and analyzed by flow cytometry (FACSCaliber, BD Biosciences).

Cell viability in *prmt2*$^{+/+}$ and *prmt2*$^{-/-}$ MEFs after etoposide exposure was analyzed as follows. Cells were seeded at 2.5×10^5 per well in six-well plates and 12 h later were transfected with control PRMT2 expression plasmids. At 24 h after transfection, cells were stimulated with etoposide (100 μM) for 24 h. Cells were then treated with trypsin and stained with trypan blue (Invitrogen). Unstained surviving cells were counted with a hemocytometer. The net difference in survival cell number between the untreated group and the etoposide group was treated as dead cells, and cell death rate was calculated as a ratio of the number of dead cells versus the number of untreated cells. Apoptosis caused by etoposide was confirmed by microscopic observation by FITC-annexin V staining according to the manufacturer's instructions (Annexin V FITC Apoptosis Detection kit; Calbiochem).

RESULTS

To determine whether PRMT1, -2, and -3 could affect NF-κB function, their potential to regulate effects on κB transcription was examined. Sequence comparison of the arginine methyltransferases has revealed several motifs shared by these proteins (Fig. 1A, top). Transient cotransfections were performed using PRMT1, PRMT2, and PRMT3 expression plasmids with an HIV-1 reporter plasmid in the human renal epithelial cell line 293T. While PRMT1 stimulated κB transcription ~10 fold, PRMT2 inhibited transcription ~50 fold, and PRMT3 did not affect transcription of the reporter plasmid (Fig. 1A, bottom left). These results suggest that PRMT2 is unique among the PRMTs in its ability to inhibit κB-dependent transcription.

To map the domains responsible for inhibition of this tran-

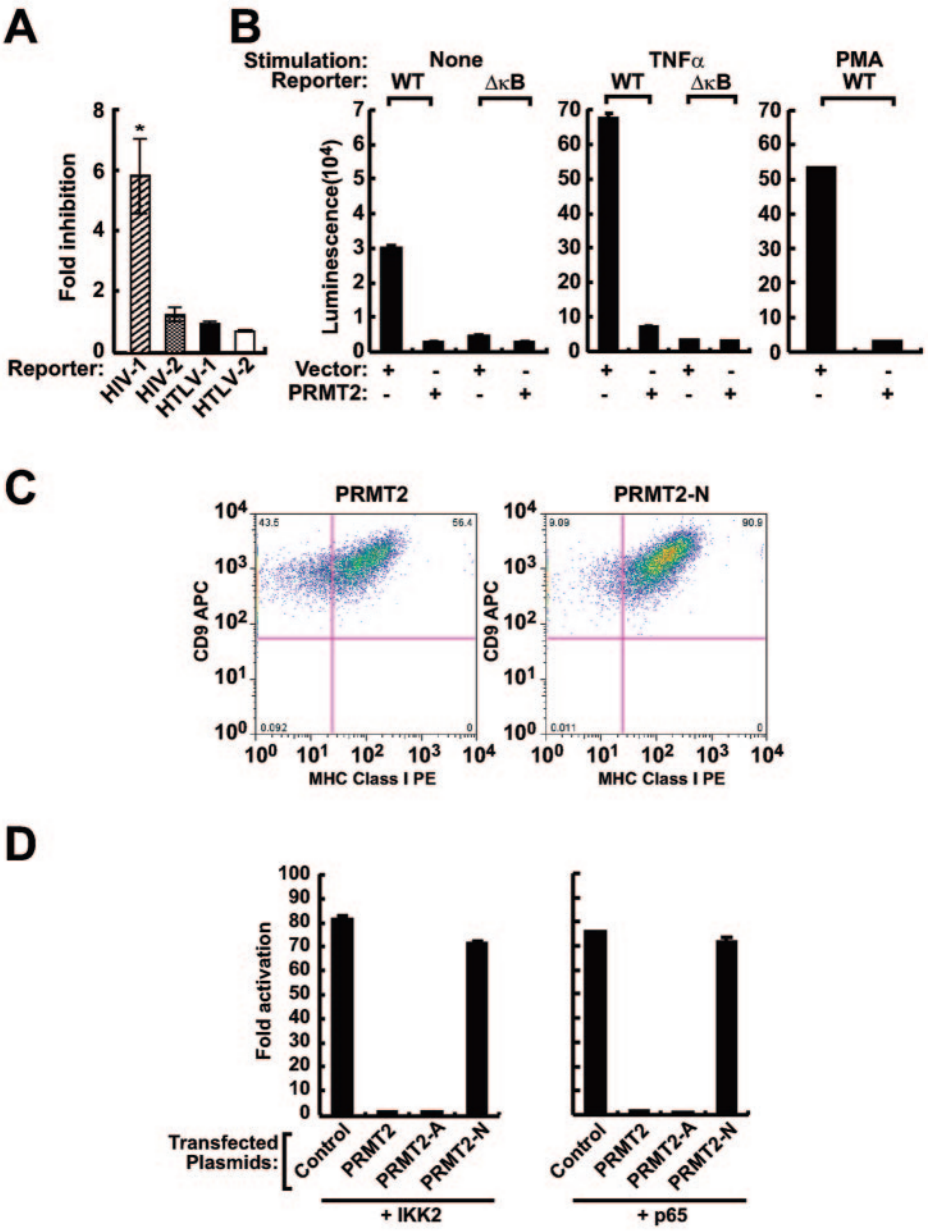

FIG. 2. Transcriptional inhibition by PRMT2 is κB dependent, and IKK-2- or p65-induced NF-κB activation is blocked by PRMT2. (A) Transcriptional inhibition by PRMT2 is promoter specific; the effect of PRMT2 on HIV and other enhancers by a CAT reporter assay was studied. 293 cells were transfected with 1 μg of the indicated reporter plasmids and 5 μg of either PRMT2 or pVR1012 plasmids. Cells were harvested 36 h posttransfection, and CAT assays were performed. Data shown are the means (±standard error of the mean [SEM]) of fold inhibition in the presence of PRMT2 over a vector control of three independent experiments. A statistically significant effect of PRMT2 on the HIV-1 promoter was noted at 5 μg (*, $P < 0.01$ compared to vector control; Student's t test). PRMT2 did not significantly inhibit transcription from the other promoters tested. (B) PRMT2 inhibits gene expression in a κB-dependent manner. 293T human embryonic kidney cells were transfected with HIV-luciferase reporter (WT) or ΔκB-luciferase reporter (ΔκB) and PRMT2 or control vector plasmid. At 24 h after transfection, cells were treated with vehicle (left) or with TNF-α (20 ng/ml) (middle) or PMA (10 ng/ml) (right) as indicated, and luciferase activity was measured 48 h posttransfection. (C) PRMT2 inhibits expression of endogenous MHC-I, an NF-κB-dependent endogenous gene. 293T cells were transfected with HA-PRMT2 or HA-PRMT2-N. Transfected cells were detached after 48 h and analyzed by flow cytometry for MHC-I and CD9 in HA-positive cells in PRMT2-transfected (left) or PRMT2-N-transfected (right) cells. (D) NF-κB induction by IKK2 or p65 is efficiently blocked by PRMT2. 293T cells were transfected with plasmids as indicated, and the κB-luciferase reporter gene was used to monitor NF-κB activity 48 h after transfection. Values are expressed as fold stimulation compared to the control vector.

scription, truncation and point mutations were made in PRMT2 (Fig. 1B, top) and cotransfected with an NF-κB reporter in 293T cells. PRMT2-A represents an alternatively spliced form of PRMT2 found in the expressed sequence tag database. This isoform contains the first 218 amino acids of PRMT2 and differs from full-length PRMT2 by the absence of the less-conserved COOH-terminal domain. PRMT2-N was generated by introducing a stop codon after amino acid 95

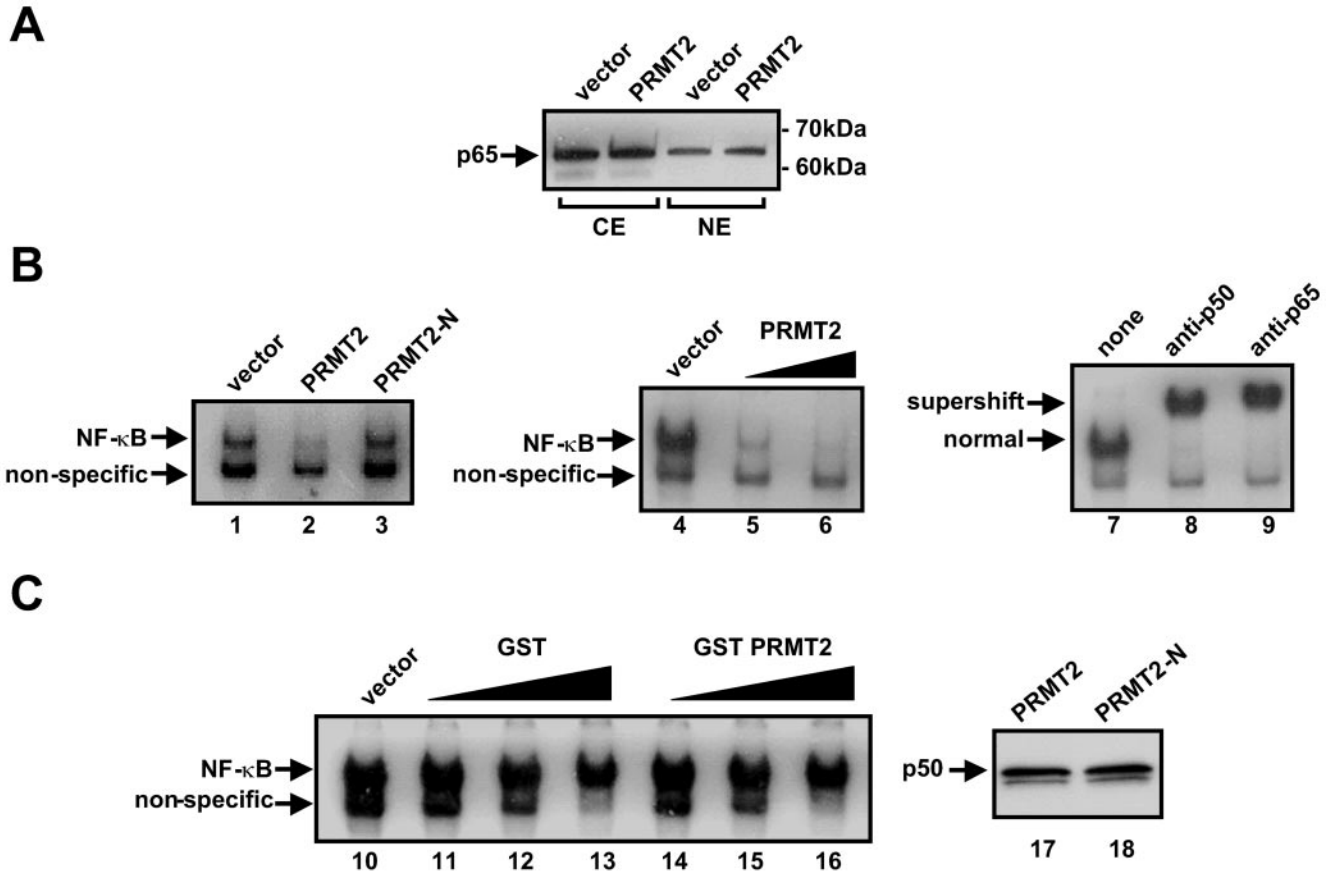

FIG. 3. PRMT2 does not interfere with p50/p65 dimerization or DNA binding. (A) PRMT2 does not alter p65 expression or localization. A total of 10 μg of cytoplasmic (CE) or nuclear (NE) extract from 293 cells transfected with vector and PRMT2 expression vectors was subjected to 4 to 15% SDS-PAGE and transferred to a PVDF membrane. The membrane was probed with an antibody to RelA (p65). (B) The effect of PRMT2 on NF-κB DNA binding was assayed by analyzing DNA-binding activity of nuclear extracts from 293 cells cotransfected with NF-κB1 (p50)/RelA (p65) and PRMT2 or PRMT2-N expression vectors (lanes 1 to 3). PRMT2 inhibited p50/p65 DNA binding in a dose-dependent manner (lanes 5 and 6), and the shifted complex contained p50/p65 (lanes 8 and 9). At 36 h after transfection, nuclear extracts were made and analyzed by EMSA with a ^{32}P-labeled double-stranded oligonucleotide containing NF-κB-binding sites. NF-κB DNA-binding activity was measured from nuclear extracts from 293 cells cotransfected with NF-κB1/RelA and vector control (5 μg) (lane 4) or increasing amounts (2.5 and 5 μg) (lanes 5 and 6) of PRMT2 expression vector. EMSAs were performed as before, but antibodies to NF-κB were included in the reaction mixture to confirm the nature of the retarded complexes. The complex was supershifted by both p50 and p65 antibodies, confirming its identity as NF-κB (lanes 7 to 9). (C) PRMT2 does not inhibit NF-κB DNA binding (left). Increasing amounts of GST (lanes 11 to 13) or GST-PRMT2 (lanes 14 to 16) were added to p52/p65-transfected 293 extracts prior to the addition of the labeled probe to the reaction mixture. EMSAs were carried out as before. No inhibition of NF-κB DNA binding was seen in the presence of GST-PRMT2. PRMT2 does not disrupt p50/p65 complex formation (lanes 17 and 18). Immunoprecipitations were carried out from PRMT2- or PRMT2-N transfected 293 whole-cell extracts with a p65 antibody. p50 coimmunoprecipitated with p65 was detected by Western blotting with an anti-p50 antibody. No difference was detected in the amount of p50 brought down in the presence of PRMT2 or PRMT2-N, suggesting that PRMT2 does not disrupt p50/p65 complex formation.

before the putative Ado-Met domain of PRMT2. To analyze the role of the Ado-Met domain further, another mutant, PRMT2-4A, was prepared in which the sequence $_{141}$ILDV$_{144}$ was altered to four consecutive alanines to compare the effects of point mutations in this highly conserved region. Under conditions in which PRMT2, PRMT2-A, and PRMT2-4A inhibited NF-κB activity, PRMT2-N did not (Fig. 1B, bottom left), suggesting that a structural, but not necessarily a functional, methyltransferase domain is required for transcriptional inhibition.

The HIV-1 long terminal repeat contains two highly conserved κB-binding sites that play an important regulatory role in HIV-1 gene expression (37). To study the effect of PRMT2 on transcription, PRMT2 was cotransfected with HIV-1, HIV-2, human T-cell lymphotropic virus type 1 (HTLV-1), or HTLV-2 reporter plasmids into 293 cells. Despite the presence of a single κB site in HIV-2, its expression shows greater dependency on Ets family transcription factors (30). No significant reduction was seen with either HIV-2 or HTLV reporter plasmids, while HIV-1 chloramphenicol acetyltransferase (CAT) expression was substantially inhibited, documenting the specificity of PRMT2 (Fig. 2A). To determine its dependence on NF-κB, HIV-1 reporter plasmids with WT or mutant (ΔκB) sites were cotransfected transiently with control or PRMT2 expression plasmids. PRMT2 significantly inhibited both basal and TNF-α-dependent HIV-1 transcription from the wild type but not the κB-mutant reporter in 293 renal epithelial cell lines (Fig. 2B, left and middle). The κB effect was dose dependent

and was also observed with other inducers of NF-κB, including phorbol myristic acid (PMA) (Fig. 2B, right). These results suggested that PRMT2 could block NF-κB activation from various stimuli. PRMT2 was also able to modulate the expression of endogenous κB-regulated genes. PRMT2 transfection of 293T cells decreased endogenous major histocompatibility complex class I (MHC-I) cell surface expression by flow cytometry, in contrast to CD9, which is an NF-κB-independent gene (Fig. 2C).

The mechanism and site of action of PRMT2 in the NF-κB signaling pathway was further defined by cotransfection of PRMT2 and its mutants with different regulators in this pathway with an NF-κB reporter in 293T cells (Fig. 2D). PRMT2 and PRMT2-A inhibited both IKK2- and p65-induced NF-κB activity (Fig. 2D; see Fig. S1 in the supplemental material), while PRMT2N was unable to block this effect (Fig. 2D), suggesting that PRMT2 exerted its inhibitory action on nuclear NF-κB rather than by modulation of cytoplasmic IκB or the IκB kinase complex.

To investigate this mechanism further, p65 expression levels and cellular localization of RelA and IκB were examined. Immunoblotting for RelA in cytoplasmic and nuclear extracts from 293 cells transfected with PRMT2 revealed no effect on RelA protein levels or on its subcellular localization (Fig. 3A). Thus, PRMT2 appeared to affect RelA function without altering its nuclear accumulation, for example, by interfering with its DNA-binding activity. To determine whether PRMT2 could affect nuclear NF-κB DNA-binding activity, PRMT2 was cotransfected into 293 cells with the NF-κB1 (p50) and RelA (p65) expression vectors. Analysis of nuclear extracts from transfected cells by mobility shift assays, using a consensus κB-binding site double-stranded oligonucleotide, showed that PRMT2 inhibited DNA binding of the p50/p65 complex in a dose-dependent manner (Fig. 3B, lanes 2, 5, and 6). In contrast, the inactive PRMT2-N mutant did not affect NF-κB DNA binding (Fig. 3B, lane 3). The nature of these complexes was confirmed by supershifts with antibodies directed against p50 and p65 (Fig. 3B, lanes 8 and 9).

To examine whether PRMT2 directly affected NF-κB DNA binding, a recombinant GST PRMT2 fusion protein, GST-PRMT2, was added to the gel shift reaction mixture. No decrease in DNA binding over GST control was observed (Fig. 3C, lanes 14 to 16), suggesting that the inhibition of NF-κB DNA binding in PRMT2-transfected extracts was indirect. Because p50/p65 dimerization is important for efficient NF-κB DNA binding (44), PRMT2 might inhibit DNA binding by antagonizing p50/p65 complex formation. To test this possibility, p50/p65 complexes were immunoprecipitated from PRMT2-transfected 293 cell nuclear extracts with an anti-p65 antibody. Western blotting for p50 showed that equal amounts of p50 coimmunoprecipitated with p65 from cells transfected with PRMT2 or PRMT2-N (Fig. 3C, lanes 17 and 18), suggesting that decreased NF-κB DNA binding in PRMT2-transfected cell extracts was not due to interference with p50/p65 dimerization. In this assay, PRMT2 also did not affect interactions of p65 with p300 and the general transcriptional machinery (see Fig. S2A in the supplemental material), nor did it catalyze the methylation of histones (see Fig. S2B in the supplemental material), p65, p50, IκB, hnRNPU, and CRM1 in both bacterially purified and cell extract-immunoprecipitated PRMT2 by an in vitro methyltransferase assay (data not shown). Whole-cell hypomethylated extracts from PRMT2-transfected cells showed minimal changes in methylation when incubated in vitro with [*methyl*-^{3}H]*S*-adenosyl-L-methionine over control, while PRMT1-transfected extracts were hypermethylated (see Fig. S2C in the supplemental material). Taken together, these data suggest that the methyltransferase function of PRMT2 is not necessary for inhibiting NF-κB activity.

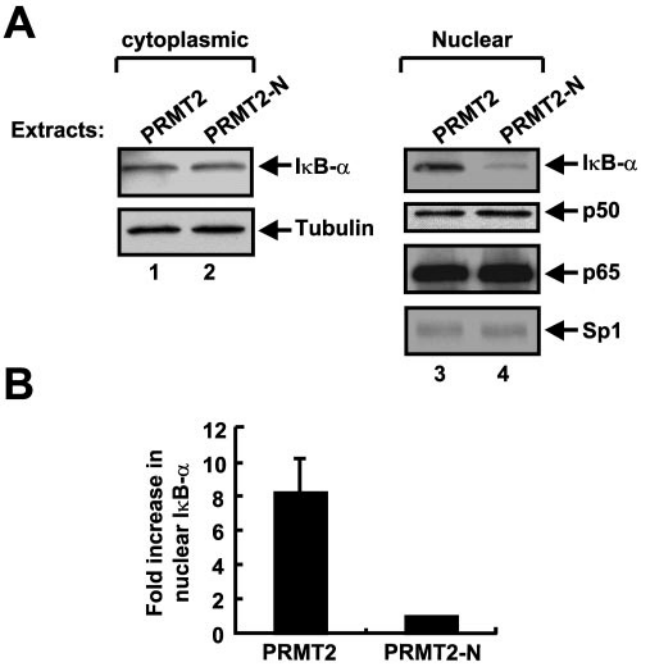

FIG. 4. PRMT2 promotes nuclear accumulation of IκB-α. (A) Cells were stimulated with TNF-α (200 U/ml) 24 h after transfection and harvested at 36 h. A total of 10 μg of cytoplasmic extracts was resolved by 4 to 15% SDS-PAGE and transferred to a PVDF membrane. Immunoblotting was done with an anti-IκB-α antibody. The membrane was then stripped and reprobed using an antibody to tubulin. Cytoplasmic IκB-α levels remain unchanged in the presence of PRMT2 or PRMT2-N (lanes 1 and 2). Increased IκB-α protein levels in nuclear extracts from PRMT2-transfected cells were observed (lane 3). Little or no IκB-α in nuclear extracts from PRMT2-N-transfected cells was seen (lane 4). (B) Blots were stripped and reprobed with antibodies to RelA (p65), p50, or Sp1 (middle and lower right). Nuclear IκB-α protein levels are increased ~8-fold in PRMT2-transfected cells over the mutant control (Fig. 4A, right top). Film images were digitized using a scanner, and the bands were quantified with Imagequant software. Data are expressed as the means (±SEM) fold increase in nuclear IκB-α from three independent experiments.

Newly synthesized IκB-α can be detected in the cytoplasm but also in the nucleus, where it associates with NF-κB/RelA complexes. As newly synthesized IκB-α accumulates in the nucleus, there is a progressive reduction of both NF-κB DNA binding and NF-κB-dependent transcription (4), presumably by export of NF-κB–IκB-α complexes from the nucleus (3, 42, 49). PRMT2 could therefore potentially affect nuclear IκB-α levels, resulting in decreased NF-κB DNA binding. To examine whether PRMT2 increased nuclear IκB-α levels, nuclear and cytoplasmic extracts were prepared from PRMT2 or inactive, PRMT2-N-transfected 293 cells. Immunoblotting for IκB-α and RelA proteins in the two fractions revealed no

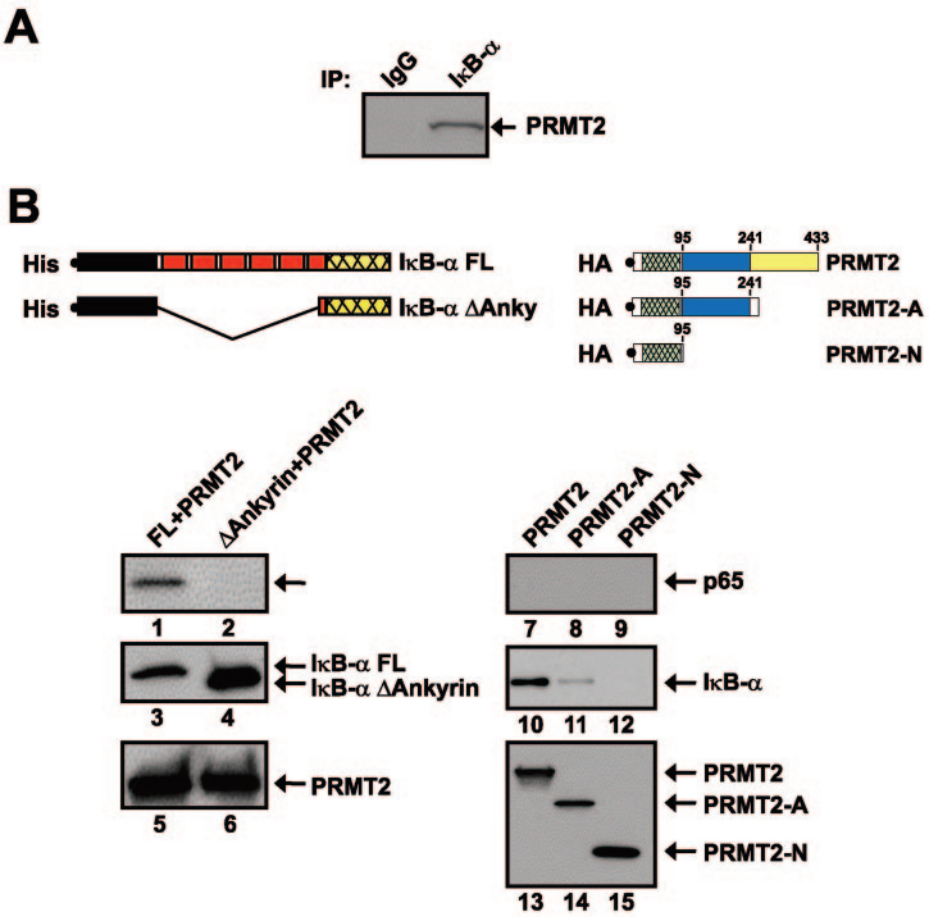

FIG. 5. PRMT2 associates with the endogenous IκB-α complex. (A) Immunoprecipitation of endogenous PRMT2-IκB-α complex. NIH 3T3 cell extracts (2 mg) were immunoprecipitated with agarose-conjugated control IgG or IκB-α antibody, resolved by 10% SDS-PAGE, and immunoblotted with antibody to PRMT2. (B) Mapping the region of IκB-α and PRMT2 interaction. A schematic representation of His-tagged IκB-α deletions (top left) and HA-tagged PRMT2 deletions (top right) is shown. The IκB-α signal recognition domain is shown in black, ankyrin repeats are shown in red, and the PEST domain is shown in yellow (top left). For PRMT2, the N-terminal domain is shown in green, and the arginine methyltransferase region, composed of an Ado-Met-binding domain in blue and the divergent C-terminal domain in yellow (top right), is shown. (Bottom) To map IκB-α domains that interacted with PRMT2, 293 cells were transfected with HA-tagged PRMT2 (top right) and His-tagged derivatives of the indicated IκB-α expression vectors (top left) as indicated. After 24 h, cells were harvested in cell lysis buffer, and cell lysates were immunoprecipitated with agarose-conjugated antibody to His (IκB-α) (lanes 1 to 4) and HA (PRMT2) (lanes 5 to 6), fractionated by SDS-PAGE, and analyzed by immunoblotting with antibody to HA (PRMT2) (lanes 1, 2, 5, and 6) and His (lanes 3 and 4). To map the region of PRMT2 that interacted with endogenous IκB-α and p65, 293 cells were transfected with HA-tagged PRMT2 (top right) derivatives as indicated. Cells were harvested 24 h after transfection in cell lysis buffer, immunoprecipitated with agarose-conjugated antibody to HA (PRMT2 and derivatives) (lanes 7 to 15), fractionated by SDS-PAGE, and analyzed by immunoblotting with antibody to p65 (lanes 7 to 9), IκB-α (lanes 10 to 12), or HA (lanes 13 to 15).

significant changes in the levels of cytoplasmic IκB-α (Fig. 4A, left, lane 1 versus lane 2) or nuclear p50 and RelA (p65) levels (Fig. 4A, right, lane 3 versus lane 4), but a distinct increase in the amount of nuclear IκB-α was observed with PRMT2-transfected cells compared to the functionally inactive PRMT2-N mutant control (Fig. 4A, right, lane 3 versus lane 4, and Fig. 4B; $P < 0.01$, PRMT2 compared to the mutant PRMT2-N using Student's t test) with cells that had been stimulated with TNF-α. This increase in the nuclear accumulation of IκB-α therefore appeared to be responsible for the PRMT2-mediated inhibition of NF-κB DNA binding and NF-κB-dependent transcription.

A polyclonal antibody to recombinant PRMT2 was used to examine the association between endogenous PRMT2 and IκB-α in vivo. Immunoprecipitation of IκB-α from NIH 3T3 cell extracts with a control or anti-IκB-α antibody, followed by immunoblotting with antibody to PRMT2, revealed that PRMT2 interacted with endogenous IκB-α (Fig. 5A) but not IκB-β (data not shown). The domain of IκB-α required for association with PRMT2 was mapped by in vivo immunoprecipitation assays where HA-tagged PRMT2 was coexpressed with truncation mutants of His-tagged IκB-α (Fig. 5B, top) in 293 cells. The ankyrin domain was necessary for this association (Fig. 5B, bottom, lanes 1 and 2). The domain of PRMT2 that interacted with endogenous IκB-α was mapped by immunoprecipitation, following expression of HA-tagged PRMT2 truncation mutants (Fig. 5B, top). IκB-α interacted with PRMT2 and PRMT2-A (Fig. 5B, bottom, lanes 10 and 11) but

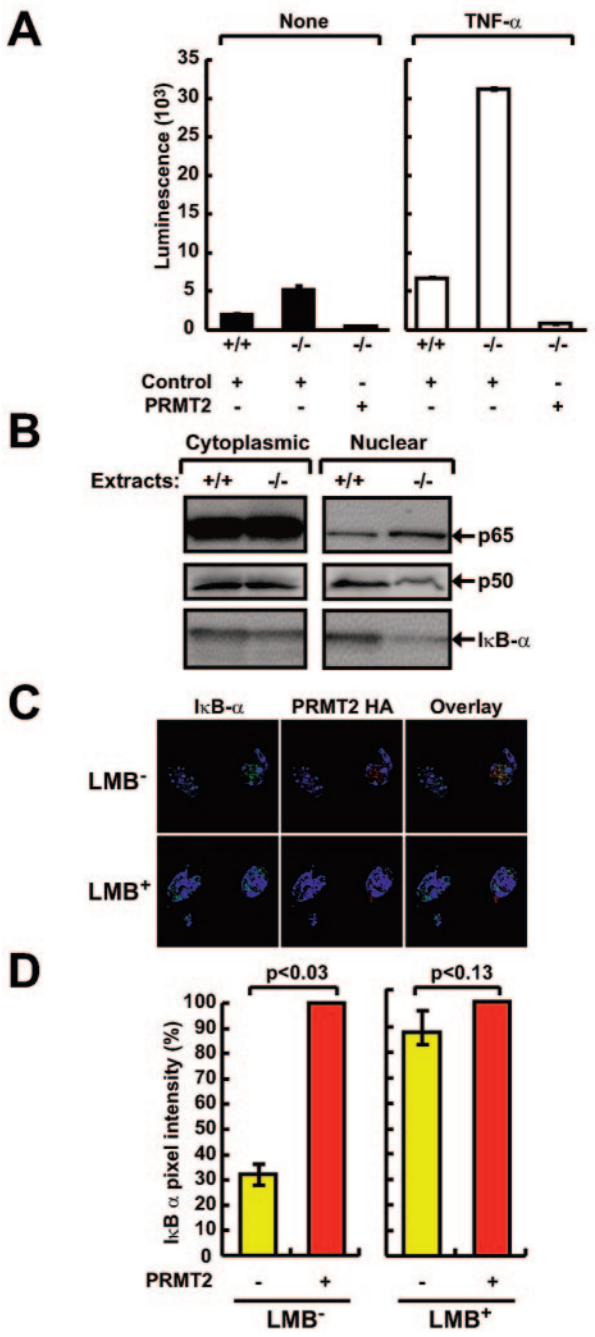

FIG. 6. Lack of NF-κB inhibition in *prmt2*$^{-/-}$ fibroblasts, reversal by complementation through transfection of PRMT2, and dependence on LMB-sensitive nuclear export. (A) NF-κB response in *prmt2*$^{-/-}$ fibroblasts or *prmt2*$^{-/-}$ fibroblasts complemented with PRMT2. *prmt2*$^{-/-}$ MEFs were transfected with a control vector or HA-tagged PRMT2 expression vector and the NF-κB reporter (5κB-luciferase). *prmt2*$^{+/+}$ MEFs transfected with control vector and the NF-κB reporter (5κB-luciferase) served as the control. Thirty hours after transfection, cells with or without TNF-α treatment (1,000 U/ml for 6 h) were harvested and analyzed with the Dual-Luciferase Reporter Assay system (Promega). *Renilla* luciferase activity by PRL-TK was used as an internal standard to control transfection efficiency, and the fold increase in activity relative to unstimulated wild-type cells is shown. Dark bars, unstimulated cells; open bars, TNF-stimulated cells. (B) *prmt2*$^{-/-}$ MEFs have less nuclear IκB-α. Cells were treated with TNF-α for 0, 15, 30, and 60 min. A total of 20 μg of cytoplasmic and nuclear extracts at the 30-min time point, optimal for induction, from *prmt2*$^{+/+}$ and *prmt2*$^{-/-}$ MEFs was resolved by 4 to 15% SDS-PAGE and transferred to a PVDF membrane. Immunoblotting was done with an anti-p65, anti-p50, and anti-IκB-α antibody. (C) PRMT2 affects nuclear export of IκB-α. *prmt2*$^{-/-}$ fibroblasts were transfected with an HA-tagged PRMT2 expression vector. At 36 h after transfection, the cells were treated with TNF-α for 30 min. The medium was removed, and cells were incubated for an additional 30 min in the absence (top) or presence (bottom) of LMB. Cells were fixed, permeabilized, and stained for IκBα (left) with Alexa 488 (green) and for HA (PRMT2) (middle) with Alexa 564 (red). Overlay of IκBα and HA (PRMT2) staining is also shown (right). The nucleus is stained with DAPI (blue). (D) Leptomycin B does not alter nuclear IκB-α in the presence of PRMT2. Experiments were done as described above. Quantification of nuclear IκBα in individual cells from several fields was done as follows. The outline of cell nuclei in a field was drawn with Leica confocal software. IκBα pixel intensity from the nucleus of each individual cell in the field was measured. The cells that had PRMT2 were distinguished by the presence of the HA tag (red). The nucleus was identified by DAPI staining. For each condition, the data from 10 fields were compiled (approximately five to six cells per field; 30% of the cells expressed PRMT2) and are presented on a graph (LMB$^-$, left; LMB$^+$, right), with *P* values as indicated.

did not associate with PRMT2-N (Fig. 5B, bottom, lane 12), indicating that the Ado-Met domain is necessary to promote IκB-α binding. When the ratios of PRMT2 or PRMT2-A binding to IκB-α were compared, both interacted with IκB-α with similar affinity. PRMT2 or the mutants did not interact with endogenous p65 (Fig. 5B, bottom, lanes 7, 8, and 9).

To determine whether similar effects would be observed in nontransformed cell lines with physiological levels of protein, NF-κB inducibility was analyzed in MEFs derived from PRMT2 null mice (T. Yoshimoto et al., unpublished data). A κB-luciferase reporter was transfected with control or PRMT2 expression plasmid into WT and *prmt2*$^{-/-}$ MEFs and incubated in the presence or absence of TNF-α. Compared to wild-type cells and consistent with the transfection results in 293 cells, *prmt2*$^{-/-}$ MEFs were more responsive to NF-κB induction by TNF-α (Fig. 6A). Complementation of *prmt2*$^{-/-}$ MEFs with PRMT2 completely abolished NF-κB induction by TNF-α (Fig. 6A). IκB-α and p65 levels in cytoplasmic and nuclear extracts from control and *prmt2*$^{-/-}$ MEFs were examined after TNF-α stimulation for 0, 15, 30, and 60 min. Immunoblotting for p65, p50, and IκB-α in the two fractions revealed no significant changes in the levels of cytoplasmic IκB-α at a representative 30-min time point (Fig. 6B, bottom left) or p50 (Fig. 6B, middle), but a moderate increase in RelA (p65) levels (Fig. 6B, top) and a distinct decrease in the amount of nuclear IκB-α was observed with *prmt2*$^{-/-}$ compared to control MEFs (Fig. 6B, bottom right).

NF-κB DNA-binding and NF-κB-dependent transcriptional activation is reduced by accumulation of newly synthesized IκB-α in the nucleus (4). NF-κB–IκBα complexes are exported from the nucleus to the cytoplasm by CRM1 (3, 42, 49), and this nuclear export can be blocked by LMB (23, 38, 49). To understand the role of PRMT2 in promoting nuclear IκBα accumulation, *prmt2*$^{-/-}$ fibroblasts were transfected with an HA-tagged PRMT2 expression vector. At 36 h after transfection, the cells were treated with TNF-α for 30 min. The medium was then removed, and cells were incubated for an ad-

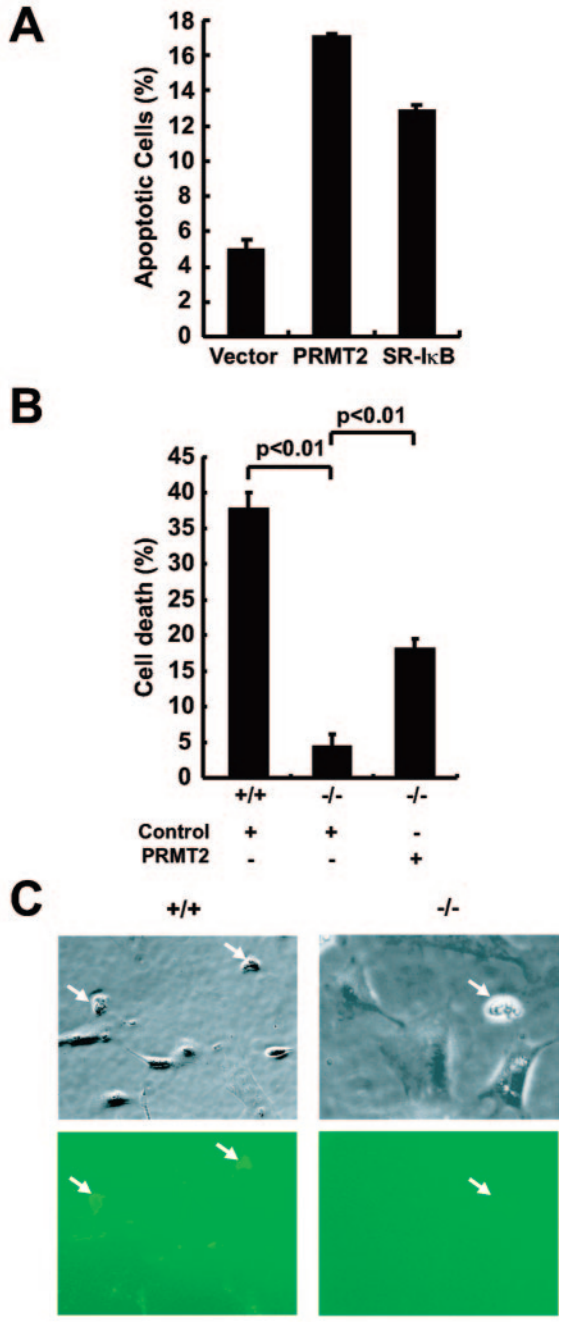

FIG. 7. *prmt2*$^{-/-}$ cells are resistant to apoptosis, and this effect can be reversed by complementing *prmt2*$^{-/-}$ cells with PRMT2. (A) PRMT2 promotes TNF-α-induced apoptosis. Empty vector, mutant IκB-α (S32A/S36A and SR-IκB), or PRMT2 plasmids were co-transfected with CD2 into 293 cells. At 24 h after transfection, cells were stimulated with TNF-α (1,000 U/ml) for 24 h. Cells were stained with antigen-presenting cell-labeled anti-CD2 antibody (BD Biosciences), annexin V, and propidium iodide and analyzed by flow cytometry (FACSCaliber; BD Biosciences). The percentages of annexin V-positive and propidium iodide-negative cells among CD2-positive cells are shown as means ± standard deviation from three different experiments. (B) Resistance of *prmt2*$^{-/-}$ MEFs to cell death after etoposide exposure. *prmt2*$^{+/+}$ and *prmt2*$^{-/-}$ MEFs (passage 4) were seeded at 2×10^5 cells per well in six-well plates. *prmt2*$^{-/-}$ MEFs were transfected with control or PRMT2 expression vector. *prmt2*$^{+/+}$ MEFs transfected with control vector served as the control. At 24 h after transfection, cells were stimulated with etoposide (100 μM) for 24 h. Cells were treated with trypsin and stained with trypan blue (Invitrogen). Unstained surviving cells were counted with a hemocytometer. Cell death represents the percentage of treated cells that underwent apoptosis relative to untreated cells. Results are shown as the mean ± SEM of three independent experiments. (C) Etoposide-induced apoptosis in *prmt2*$^{+/+}$ compared to *prmt2*$^{-/-}$ MEFs. Bright-field and fluorescent microscopy of *prmt2*$^{+/+}$ and *prmt2*$^{-/-}$ MEFs stained with FITC-labeled annexin V (magnification, ×16). Arrows indicate representative cells in light and dark fields.

ditional 30 min in the presence or absence of LMB. Cells were fixed, permeabilized, and stained for IκB-α (Fig. 6C, left) and HA (PRMT2) (Fig. 6C, middle). Confocal microscopy performed on the cells showed IκB-α accumulation in the nucleus in the presence of PRMT2 (Fig. 6C, top left and right), which did not change in the presence of LMB (Fig. 6C, bottom left and right).

To demonstrate the effect of PRMT2 further, nuclear IκB-α (Fig. 6D) was quantified in *prmt2*$^{-/-}$ fibroblasts and *prmt2*$^{-/-}$ fibroblasts complemented with PRMT2 in the presence or absence of LMB. Briefly, to quantitate the effect of PRMT2 on nuclear IκB-α, *prmt2*$^{-/-}$ fibroblasts were transfected with a control or HA-tagged PRMT2. At 36 h after transfection, cells were first treated with TNF-α for 30 min, washed, and then treated with LMB or vehicle for 30 min. Cells were fixed, permeabilized, and stained with IκB-α (green), PRMT2 (red), and DAPI (blue). Outlines of nuclei of cells with or without PRMT2 from each field of vehicle or LMB-treated cells were drawn with Leica confocal software. IκB-α pixel intensity from the nucleus of each individual cell in the field was measured using this software. In each field, the cells with PRMT2 were identified by the presence of the HA tag (red). The nuclear outline was defined by DAPI staining (blue). For each condition, the data from 10 fields were compiled (approximately five to six cells per field; 30% of the cells expressed PRMT2) and presented graphically, with *P* values as indicated. Vehicle- and LMB-treated cells are shown (Fig. 6D, left and right, respectively). LMB promoted nuclear accumulation of IκB-α in the absence of PRMT2, and transfection of PRMT2 exerted the same effect. Together, these data are consistent with the hypothesis that PRMT2 inhibits the nuclear export of IκB-α through an LMB-sensitive CRM1 pathway. At the same time, we cannot exclude the possibility that these effects are coincidental and induced by an alternative mechanism yet to be defined.

Since PRMT2 inhibits NF-κB activity, which can regulate apoptosis in some cell types (7, 51, 54), the ability of PRMT2 to independently regulate programmed cell death was next examined. Transfection of PRMT2 into 293 cells increased their susceptibility to TNF-induced cell death, comparable to levels observed with a mutant, stabilized, or superrepressor IκB (designated SR-IκB) (Fig. 7A) (7, 53, 54). To evaluate the effect of PRMT2 on programmed cell death, wild-type, knockout PRMT2 MEF or knockout MEF cells complemented with PRMT2 were exposed to etoposide, a DNA-damaging agent with proapoptotic activity. Wild-type and PRMT2-complemented MEFs displayed a substantial increase in etoposide-induced cell death and annexin V staining compared to PRMT2-deficient cells (Fig. 7B and C).

DISCUSSION

The diverse effects of protein methylation on cell function have recently become evident. In this report, PRMT2, a family member whose effects are not fully known, has been shown to regulate factors that influence cell activation and programmed cell death. PRMT2 negatively regulates κB-dependent transcription and renders cells more susceptible to apoptotic stimuli. The transcriptional effect on NF-κB is specific to PRMT2, and it is mediated through nuclear accumulation of IκB-α. Following NF-κB activation, newly synthesized IκB-α molecules enter the nucleus to remove NF-κB from DNA (3, 9, 11, 48) and with the help of its leucine-rich nuclear export sequences to transport NF-κB back to the cytoplasm (4, 42). The mechanisms involving the nuclear shuttling of NF-κB–IκB-α are unclear. While CRM1 is a facilitator of NF-κB–IκB-α nuclear export (49), proteins that inhibit nuclear export are still largely unknown. Arginine methyltransferases have been previously shown to play a role in nucleocytoplasmic transport (2). IκB-α (and not IκB-β) is known to shuttle NF-κB, and PRMT2 only interacts with IκB-α by associating with its ankyrin domain. The ankyrin domain also mediates IκB-α interaction with NF-κB. Twenty to 30% of total IκB-α is associated with PRMT2, and the affinity of IκB-α to NF-κB is predicted from our immunoprecipitation studies to be much higher than for PRMT2. Therefore, it is unclear whether a PRMT2–IκB-α complex can directly inhibit NF-κB DNA binding, but gel retardation assays performed on PRMT2-transfected 293 cell extracts (Fig. 3B, lanes 4 to 6) show that PRMT2 inhibits NF-κB DNA binding in a dose-dependent fashion. From this data, we can infer that PRMT2–IκB-α complexes still bind NF-κB subunits and prevent them from binding to DNA. This effect is likely indirect, mediated by a protein-protein interaction between the PRMT2 Ado-Met domain and IκB-α ankyrin repeats that block interaction with this export complex, since we were unable to detect altered methylation of CRM-1, hnRNPU, IκB-α, or other regulators by PRMT2 (see Fig. S2 in the supplemental material).

PRMT family members also affect transcriptional regulation through their effects on transcription coactivators, in the case of PRMT1 and PRMT4 or CARM1 (10, 28, 57), and through their ability to methylate histones H3 and H4 (6, 55). PRMT2 has been reported to be a coactivator of estrogen receptor alpha, but its mechanism of action is unclear (41). These effects suggest their involvement in chromatin remodeling. Although PRMT2 has a conserved Ado-Met domain that mediates the methyl transferase activity in PRMTs, our data show that PRMT2 is unable to methylate histones or disrupt p65 interactions with p50, p300, and TAFII250 in cells (see Fig. S2 in the supplemental material) (37), suggesting that general transcriptional machinery or chromatin remodeling is not affected by PRMT2. Overexpression of PRMT2 leads to hypomethylation of total-cell extracts compared to a mutant PRMT2-4A (see Fig. S2C in the supplemental material); amino acids ILDV, responsible for methyltransferase activity, were altered to four consecutive alanines. Since PRMT family members are known to form complexes with each other, the data could indicate that PRMT2 interacts through the Ado-Met domain to inhibit methylation of another PRMT. It may also be that the substrate for PRMT2 is yet to be identified.

This study identifies the effects of PRMT2 on a transcription factor central to cell activation and viability. Collectively, these results suggest the divergent mechanisms of transcriptional regulation by different PRMTs. PRMT2 may affect this response in part through its effects on NF-κB. The suppression of apoptosis by NF-κB is an important component of TNF-α, and DNA-damaging agents induced apoptosis dependent on induction of antiapoptotic genes (7, 26, 33, 54). NF-κB-deficient epithelial cells show increased sensitivity to DNA-damaging chemotherapeutic agents and ionizing radiation. Many epithelial and lymphoid tumors show constitutive activation of NF-κB, and it is likely that the antiapoptotic function of NF-κB represents a major obstacle to successful cancer therapy (26, 54). Although PRMT2 likely regulates apoptosis in part through its effects on NF-κB, the involvement of additional mechanisms cannot be excluded. The present study nonetheless suggests that PRMT2 affects a transcription pathway central to cell activation and cell survival.

ACKNOWLEDGMENTS

We thank Roland Kwok, Susan Farrell, Jacques Friborg, Yongnian Sun, Maria Athanassiou, J. J. Chen, and Steven King for helpful discussions and comments; Owen Schwartz and Juraj Kabat for help with confocal microscopy; Ati Tislerics and Tina Suhana for manuscript preparation; and Nancy Barrett, Karen Stroud, Toni Miller, and Brenda Hartman for preparation of figures.

N.C.M. was supported by the Cellular and Molecular Biology Program, University of Michigan. This research was supported in part by the Intramural Research Program of the NIH, specifically, the Vaccine Research Center, NIAID, and the Division of Intramural Research, NHLBI.

We have no financial or other relationships relevant to this study.

REFERENCES

1. **Agalioti, T., S. Lomvardas, B. Parekh, J. Yie, T. Maniatis, and D. Thanos.** 2000. Ordered recruitment of chromatin modifying and general transcription factors to the IFN-β promoter. Cell **103:**667–678.
2. **Aletta, J. M.** 1998. Protein methylation: a signal event in post-translational modification. Trends Biochem. Sci. **23:**89–91.
3. **Arenzana-Seisdedos, F., J. Thompson, M. S. Rodriguez, F. Bachelerie, D. Thomas, and R. T. Hay.** 1995. Inducible nuclear expression of newly synthesized IκB-α negatively regulates DNA-binding and transcriptional activity of NF-κB. Mol. Cell. Biol. **15:**2689–2696.
4. **Arenzana-Seisdedos, F., P. Turpin, M. Rodriguez, D. Thomas, R. T. Hay, J. L. Virelizier, and C. Dargemont.** 1997. Nuclear localization of IκB-α promotes active transport of NF-κB from the nucleus to the cytoplasm. J. Cell Sci. **110:**369–378.
5. **Baldwin, A. S., Jr.** 2001. The transcription factor NF-κB and human disease. J. Clin. Investig. **107:**3–6.
6. **Bauer, U. M., S. Daujat, S. J. Nielsen, K. Nightingale, and T. Kouzarides.** 2002. Methylation at arginine 17 of histone H3 is linked to gene activation. EMBO Rep. **3:**39–44.
7. **Beg, A. A., and D. Baltimore.** 1996. An essential role for NF-κB in preventing TNF-α-induced cell death. Science **274:**782–789.
8. **Ben-Neriah, Y.** 2002. Regulatory functions of ubiquitination in the immune system. Nat. Immunol. **3:**20–26.
9. **Brown, K., S. Park, T. Kanno, G. Franzoso, and U. Siebenlist.** 1993. Mutual regulation of the transcription activator NF-κB and its inhibitor IkB-α. Proc. Natl. Acad. Sci. USA **90:**2532–2536.
10. **Chen, D., H. Ma, H. Hong, S. S. Koh, S.-M. Huang, B. T. Schurter, D. W. Aswad, and M. R. Stallcup.** 1999. Regulation of transcription by a protein methyltransferase. Science **284:**2174–2177.
11. **Chiao, P. J., S. Miyamoto, and I. M. Verma.** 1994. Autoregulation of IκB-α activity. Proc. Natl. Acad. Sci. USA **91:**28–32.
12. **Covic, M., P. O. Hassa, S. Saccani, C. Buerki, N. I. Meier, C. Lombardi, R. Imhof, M. T. Bedford, G. Natoli, and M. O. Hottiger.** 2005. Arginine methyltransferase CARM1 is a promoter-specific regulator of NF-κB-dependent gene expression. EMBO J. **24:**85–96.
13. **Danthinne, X., K. Aoki, A. L. Kurachi, G. J. Nabel, and E. G. Nabel.** 1998. Combination gene delivery of the cell-cycle inhibitor p27 with thymidine kinase enhances prodrug cytotoxicity. J. Virol. **72:**9201–9207.
14. **Dignam, J. D., R. M. Lebovitz, and R. G. Roeder.** 1983. Accurate transcrip-

tion initiation by RNA polymerase II in a soluble extract from isolated mammalian nuclei. Nucleic Acids Res. **11:**1475–1489.
15. **Duckett, C. S., N. D. Perkins, T. F. Kowalik, R. M. Schmid, E.-S. Huang, A. S. Baldwin, Jr., and G. J. Nabel.** 1993. Dimerization of NF-KB2 with RelA(p65) regulates DNA binding, transcriptional activation, and inhibition by an IκB-α (MAD-3). Mol. Cell. Biol. **13:**1315–1322.
16. **Frankel, A., N. Yadav, J. Lee, T. L. Branscombe, S. Clarke, and M. T. Bedford.** 2002. The novel human protein arginine *N*-methyltransferase PRMT6 is a nuclear enzyme displaying unique substrate specificity. J. Biol. Chem. **277:**3537–3543.
17. **Ganesh, L., E. Burstein, A. Guha-Niyogi, M. K. Louder, J. R. Mascola, L. W. Klomp, C. Wijmenga, C. S. Duckett, and G. J. Nabel.** 2003. The gene product Murr1 restricts HIV-1 replication in resting CD4+ lymphocytes. Nature **426:**853–857.
18. **Gary, J. D., and S. Clarke.** 1998. RNA and protein interactions modulated by protein arginine methylation. Prog. Nucleic Acid Res. Mol. Biol. **61:**65–131.
19. **Gerritsen, M. E., A. J. Williams, A. S. Neish, S. Moore, Y. Shi, and T. Collins.** 1997. CREB-binding protein/p300 are transcriptional coactivators of p65. Proc. Natl. Acad. Sci. USA **94:**2927–2932.
20. **Goodman, R. H., and S. Smolik.** 2000. CBP/p300 in cell growth, transformation, and development. Genes Dev. **14:**1553–1577.
21. **Gros, L., C. Delaporte, S. Frey, J. Decesse, B. R. Saint-Vincent, L. Cavarec, A. Dubart, A. V. Gudkov, and A. Jacquemin-Sablon.** 2003. Identification of new drug sensitivity genes using genetic suppressor elements: protein arginine *N*-methyltransferase mediates cell sensitivity to DNA-damaging agents. Cancer Res. **63:**164–171.
22. **Hassa, P. O., C. Buerki, C. Lombardi, R. Imhof, and M. O. Hottiger.** 2003. Transcriptional coactivation of nuclear factor-κB-dependent gene expression by p300 is regulated by poly(ADP)-ribose polymerase-1. J. Biol. Chem. **278:**45145–45153.
23. **Huang, T. T., and S. Miyamoto.** 2001. Postrepression activation of NF-κB requires the amino-terminal nuclear export signal specific to IκBα. Mol. Cell. Biol. **21:**4737–4747.
24. **Kagan, R. M., and S. Clarke.** 1994. Widespread occurrence of three sequence motifs in diverse *S*-adenosylmethionine-dependent methyltransferases suggests a common structure for these enzymes. Arch. Biochem. Biophys. **310:**417–427.
25. **Karin, M., and Y. Ben-Neriah.** 2000. Phosphorylation meets ubiquitination: the control of NF-κB activity. Annu. Rev. Immunol. **18:**621–663.
26. **Karin, M., and A. Lin.** 2002. NF-κB at the crossroads of life and death. Nat. Immunol. **3:**221–227.
27. **Katsanis, N., M. L. Yaspo, and E. M. Fisher.** 1997. Identification and mapping of a novel human gene, HRMT1L1, homologous to the rat protein aginine N-methyltransferase 1 (PRMT1) gene. Mamm. Genome **8:**526–529.
28. **Koh, S. S., D. Chen, Y. H. Lee, and M. R. Stallcup.** 2001. Synergistic enhancement of nuclear receptor function by p160 coactivators and two coactivators with protein methyltransferase activities. J. Biol. Chem. **276:** 1089–1098.
29. **Lee, J. H., J. R. Cook, Z. H. Yang, O. Mirochnitchenko, S. I. Gunderson, A. M. Felix, N. Herth, R. Hoffmann, and S. Pestka.** 2005. PRMT7, a new protein arginine methyltransferase that synthesizes symmetric dimethylarginine. J. Biol. Chem. **280:**3656–3664.
30. **Leiden, J. M., C. Y. Wang, B. Petryniak, D. M. Markovitz, G. J. Nabel, and C. B. Thompson.** 1992. A novel Ets-related transcription factor, Elf-1, binds to human immunodeficiency virus type 2 regulatory elements that are required for inducible *trans*-activation in T cells. J. Virol. **66:**5890–5897.
31. **Leung, K., and G. J. Nabel.** 1988. HTLV-I transactivator induces interleukin-2 receptor expression through an NF-κB-like factor. Nature **333:**776–778.
32. **Lin, W. J., J. D. Gary, M. C. Yang, S. Clarke, and H. R. Herschman.** 1996. The mammalian immediate-early TIS21 protein and the leukemia-associated BTG1 protein interact with a protein-arginine *N*-methyltransferase. J Biol. Chem. **271:**15034–15044.
33. **Liu, Z.-G., H. Hsu, D. V. Goeddel, and M. Karin.** 1996. Dissection of TNF receptor 1 effector functions: JNK activation is not linked to apoptosis while NF-κB activation prevents cell death. Cell **87:**565–576.
34. **Markovitz, D. M., M. Hannibal, V. L. Perez, C. Gauntt, T. M. Folks, and G. J. Nabel.** 1990. Differential regulation of human immunodeficiency viruses: a novel HIV-2 regulatory element responds to stimulation of the T-cell antigen receptor. Proc. Natl. Acad. Sci. USA **87:**9098–9102.
35. **Merika, M., and D. Thanos.** 2001. Enhanceosomes. Curr. Opin. Genet. Dev. **11:**205–208.
36. **Merika, M., A. J. Williams, G. Chen, T. Collins, and D. Thanos.** 1998. Recruitment of CBP/p300 by the IFN beta enhanceosome is required for synergistic activation of transcription. Mol. Cell **1:**277–287.
37. **Nabel, G., and D. Baltimore.** 1987. An inducible transcription factor activates expression of human immunodeficiency virus in T cells. Nature **326:** 711–713.
38. **Ossareh-Nazari, B., F. Bachelerie, and C. Dargemont.** 1997. Evidence for a role of CRM1 in signal-mediated nuclear protein export. Science **278:**141–144.
39. **Perkins, N. D., L. K. Felzien, J. C. Betts, K. Leung, D. H. Beach, and G. J. Nabel.** 1997. Regulation of NF-κB by cyclin-dependent kinases associated with the p300 co-activator. Science **275:**523–527.
40. **Pollack, B. P., S. V. Kotenko, W. He, L. S. Izotova, B. L. Barnoski, and S. Pestka.** 1999. The human homologue of the yeast proteins Skb1 and Hs17p interacts with Jak kinases and contains protein methyltransferase activity. J Biol. Chem. **274:**31531–31542.
41. **Qi, C., J. Chang, Y. Zhu, A. V. Yeldandi, S. M. Rao, and Y. J. Zhu.** 2002. Identification of protein arginine methyltransferase 2 as a coactivator for estrogen receptor alpha. J. Biol. Chem. **277:**28624–28630.
42. **Rodriguez, M. S., J. Thompson, R. T. Hay, and C. Dargemont.** 1999. Nuclear retention of IκBα protects it from signal induced degradation and inhibits nuclear factor κB transcriptional activation. J. Biol. Chem. **274:**9108–9115.
43. **Scott, H. S., S. E. Antonarakis, M. D. Lalioti, C. Rossier, P. A. Silver, and M. F. Henry.** 1998. Identification and characterization of two putative human arginine methyltransferases (HRMT1L1 and HRMT1L2). Genomics **48:** 330–340.
44. **Sen, R., and D. Baltimore.** 1986. Inducibility of kappa immunoglobulin enhancer-binding protein NF-κB by a posttranslational mechanism. Cell **47:**921–928.
45. **Silverman, N., and T. Maniatis.** 2001. NF-κB signaling pathways in mammalian and insect innate immunity. Genes Dev. **15:**2321–2342.
46. **Smith, D. B., and K. S. Johnson.** 1988. Single-step purification of polypeptides expressed in *Escherichia coli* as fusions with glutathione *S*-transferase. Gene **67:**31–40.
47. **Suh, J., F. Payvandi, L. C. Edelstein, P. S. Amenta, W. X. Zong, C. Gelinas, and A. B. Rabson.** 2002. Mechanisms of constitutive NF-κB activation in human prostate cancer cells. Prostate **52:**183–200.
48. **Sun, S. C., P. A. Ganchi, D. W. Ballard, and W. C. Greene.** 1993. NF-kappa B controls expression of inhibitor I kappa B alpha: evidence for an inducible autoregulatory pathway. Science **259:**1912–1915.
49. **Tam, W. F., L. H. Lee, L. Davis, and R. Sen.** 2000. Cytoplasmic sequestration of Rel proteins by IκBα requires CRM1-dependent nuclear export. Mol. Cell. Biol. **20:**2269–2284.
50. **Tang, J., J. D. Gary, S. Clarke, and H. R. Herschman.** 1998. PRMT3, a type-1 protein arginine N-methyltransferase that differs from PRMT1 in its oligomerization, subcellular localization, substrate specificity, and regulation. J. Biol. Chem. **273:**16935–16945.
51. **van Antwerp, D. J., S. J. Martin, T. Kafri, D. R. Green, and I. M. Verma.** 1996. Suppression of TNF-α-induced apoptosis of NF-κB. Science **274:**787–789.
52. **Verma, I. M., J. K. Stevenson, E. M. Schwarz, D. V. Antwerp, and S. Miyamoto.** 1995. Rel/NF-κB/IκB family: intimate tales of association and dissociation. Genes Dev. **9:**2723–2735.
53. **Wang, C.-Y., J. C. Cusack, R. Liu, and A. S. Baldwin.** 1999. Control of inducible chemoresistance: enhanced anti-tumor therapy through increased apoptosis by inhibition of NF-κB. Nat. Med. **5:**412–417.
54. **Wang, C.-Y., M. W. Mayo, and A. S. Baldwin.** 1996. TNF- and cancer therapy-induced apoptosis: potentiation by inhibition of NF-kB. Science **274:**784–787.
55. **Wang, H., Z. Q. Huang, L. Xia, Q. Feng, H. Erdjument-Bromage, B. D. Strahl, S. D. Briggs, C. D. Allis, J. Wong, P. Tempst, and Y. Zhang.** 2001. Methylation of histone H4 at arginine 3 facilitating transcriptional activation by nuclear hormone receptor. Science **293:**853–857.
56. **Wu, B., C. Woffendin, I. MacLachlan, and G. J. Nabel.** 1997. Distinct domains of IkB-α inhibit human immunodeficiency virus type 1 replication through NF-kB and Rev. J. Virol. **71:**3161–3167.
57. **Xu, W., H. Chen, K. Du, H. Asahara, M. Tini, B. M. Emerson, M. Montminy, and R. M. Evans.** 2001. A transcriptional switch mediated by cofactor methylation. Science **294:**2507–2511.
58. **Yamaoka, S., G. Courtois, C. Bessia, S. T. Whiteside, R. Weil, F. Agou, H. E. Kirk, R. J. Kay, and A. Israel.** 1998. Complementation cloning of NEMO, a component of the IκB kinase comple essential for NF-κB activation. Cell **93:**1231–1240.
59. **Zandi, E., D. M. Rothwarf, M. Delhase, M. Hayakawa, and M. Karin.** 1997. The IκB kinase complex (IKK) contains two kinase subunits, IKKα and IKKβ, necessary for IκB phosphorylation and NF-κB activation. Cell **91:** 243–252.